PNAS

Supporting Information for

Single-Atom Mo-Co Catalyst with Low Biotoxicity for Sustainable Degradation of High Ionization Potential Organic Pollutants

Zhuan Chen[1‡], Faliang An[2‡], Yayun Zhang[3], Zhiyan Liang[1], Wenyuan Liu[1], Mingyang Xing[1,3*]

*Mingyang Xing
mingyangxing@ecust.edu.cn

This PDF file includes:

Supporting information Text

Text S1. Experimental Section

Chemicals

$Co(CH_3COO)_2·4H_2O$; $(NH_4)_2MoO_4$; 1,10-phenanthroline; $Mg(OH)_2$; $CoCl_2·6H_2O$; NaOH; H_2SO_4; Phosphate buffer; $NaHCO_3$; Na_2SO_4; NaCl; Na_2CO_3; $NaNO_3$; Na_3PO_4; KI; Tertiary butyl alcohol (TBA); benzoquinone (p-BQ); 2,2,6,6-tetramethylpiperidine (TEMP); Dimethyl sulfoxide (DMSO); 5,5-Dimethyl-1-pyrroline N-oxide (DMPO); (E)-1,2-Diphenylethene; 2,3-Diphenyloxirane; Methyl phenyl sulfone (PMSO); Co_3O_4.

Device for Characterization

Themis Z aberration-corrected transmission electron microscope (AC-TEM), scanning electron microscope (SEM, Vega 3 TESCAN), and high-resolution transmission electron microscope (HRTEM, JEM-2100) were applied for the detailed microstructure. The Zeta potential of catalysts was measured using Zeta potential analyzer (ZEN 3700, Malvern Instruments Ltd.). Brunauer, Emmett and Teller (BET) surface areas were investigated by nitrogen adsorption at 77 K (Micromeritics ASAP2020). The elemental proportion and leaching ion concentration were tested by an inductively coupled plasma-atomic emissions spectrometer (ICP-AES, Varian 710). The pH measurement and calibration were carried out on a METTLER TOLEDO (FE28) pH meter with Le438 electrode probe sensor. Ultraviolet–visible (UV–vis) spectrophotometry (Shimadzu, UV-2450) was used to measure the concentrations of RhB, other organic dyes, PMS and salicylic acid. X-ray photoelectron spectroscopy (XPS) analysis was conducted using a Thermo Scientific K-Alpha+ with Al Kα radiation (Energy: 1486.6 eV, voltage: 15 KV, beam current: 15 mA). X-ray diffraction (XRD) measurements were performed with a Rigaku Ultima IV (Cu Ka radiation, λ = 1.5406 Å) in the range of 5°–80° (2θ). Electro-Spin Resonance Spectrometer (EMX-8/2.7) with 5, 5-Dimethyl-1-Pyrrolidine-N-oxide (DMPO) and 2, 2, 6, 6-Tetramethylplperldine (TEMP) as spin-trapping reagent was used to detect the radical in the reaction under the condition as follow: a center field of 352.0 mT, a microwave frequency of 9.880 GHz, a microwave power of 6.409 mW, and a temperature of 300.0 K. Bonding on the surface of $SAMCC_{0.5}$ and Co-N-C was detected using Fourier Transform-Infrared Spectrometer (Thermo Nicolet 7800～350/cm 0.01/cm/6700). High performance liquid chromatograph (HPLC, INESA) equipped with a diode array detector and a LC-08 C_{18} column (4.6 mm × 150 mm) was employed to analyze the concentration of pollutants. PMSO and $PMSO_2$ was detected using a mobile phase of 20% (v/v) acetonitrile aqueous solution with detection wavelength at 215 nm. (E)-1,2-Diphenylethene and 2,3-Diphenyloxirane was detected using a mobile phase of 70% (v/v) acetonitrile aqueous solution with detection wavelength at 226 nm. 4-CP, nitrobenzene and aniline were detected using a mobile phase of 70% (v/v) methanol aqueous solution with detection wavelength at 279, 262 and 244 nm. X-ray absorption spectra (XAS) were collected on SPring-8 14b2. X-ray absorption near-edge structure (XANES) and extended X-ray absorption fine structure spectra (EXAFS) data reduction and analysis were processed by Athena and hama_fortran.

Determination of PMS concentration

The concentration of remaining PMS was determined by a colorimetric method. 0.5 g $NaHCO_3$, 10 g KI and 100 mL nitrogen-blown anaerobic water were mixed as a stock solution. In a typical test, an aliquot of 5.0 mL filtrate was immediately transferred into a colorimetric tube with 5 mL stock solution at given time intervals. After 15 min the concentration of PMS was detected by a UV-vis spectrometer at 354 nm.

Detection of high valent cobalt

(E)-1,2-Diphenylethene was employed to detect the presence of high valent Co at first. 0.01 mol (E)-1,2-Diphenylethene was dissolved in 100 mL 80% acetonitrile solution (v/v) firstly. The dosage of catalyst and PMS were consistent with Fenton-like experiment. The concentration of (E)-1,2-Diphenylethene and 2,3-Diphenyloxirane were detected by HPLC. PMSO was also employed to detect the presence of high valent Co. 0.01 mol PMSO was dissolved in 100 mL deionized water. The dosage of catalyst and PMS were consistent with Fenton-like experiment. The concentration of PMSO and $PMSO_2$ were detected by HPLC.

Radical Quenching Tests

Various sacrificial agents were used to test the dominant reactive oxygen species (ROSs) in the $SAMCC_{0.5}$-PMS system. TEMP, TBA, DMSO and p-BQ were added respectively at the beginning of experiment and the other steps were the same as the catalytic activity test procedure.

Degradation Stability Test

In the cyclic experiment, all experimental processes were consistent with catalytic effect test. After each cycle, the catalyst is filtered from the reaction solution and washed with deionized water. And then catalyst is dried in a vacuum oven before next experiment cycle. For the long-term experiment, all experimental process were consistent with catalytic effect test and 200 μL 10 mg/mL phenol was added into solution whenever the phenol in a system was degraded by 90%.

Density Functional Theory (DFT) calculations

Vienna Ab Initio Package (VASP)(1,2) was employed to perform all spin-polarized density functional theory (DFT) calculations within the generalized gradient approximation (GGA) using the Perdew-Burke-Ernzerhof (PBE)(3) formulation. We have chosen the projected augmented wave (PAW) potentials(4,5) to describe the ionic cores and take valence electrons into account using a plane wave basis set with a kinetic energy cutoff of 450 eV. Partial occupancies of the Kohn−Sham orbitals were allowed using the Gaussian smearing method and a width of 0.05 eV. The electronic energy was considered self-consistent when the energy change was smaller than 10^{-5} eV. A geometry optimization was considered convergent when the energy change was smaller than 0.02 eV $Å^{-1}$. The vacuum spacing in a direction perpendicular to the plane of the structure is 18 Å. The weak interaction was described by DFT+D3 method using empirical correction in Grimme's scheme(6,7).

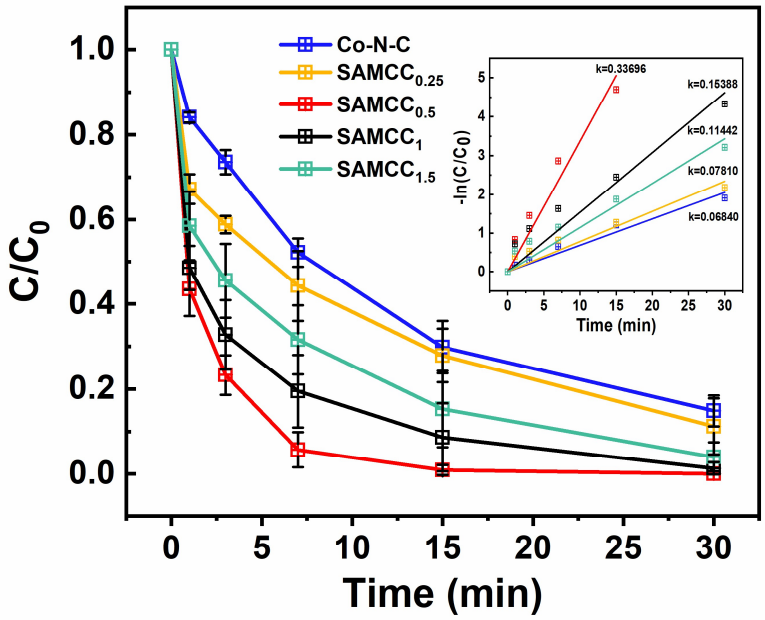

Fig. S1. Degradation activity of $SAMCC_x$ and Co-N-C Dosage: Catalyst :30 mg; PMS: 20 mg; C_{phenol}: 20 mg/L.

For the synthesis of $SAMCC_x$, the dosage of 1,10-phenanthroline and $Co(CH_3COO)_2$ was 148.5 mg and 62.5 mg. And the dosage $(NH_4)_2MoO_4$ of was 0.0005x mol. From the data in the graph, it can be concluded that the best degradation activity of the catalyst was achieved when the ratio of $(NH_4)_2MoO_4$ to $Co(Ac)_2$ was 0.25:1. At this point, the amount of $(NH_4)_2MoO_4$ was 4.9 mg.

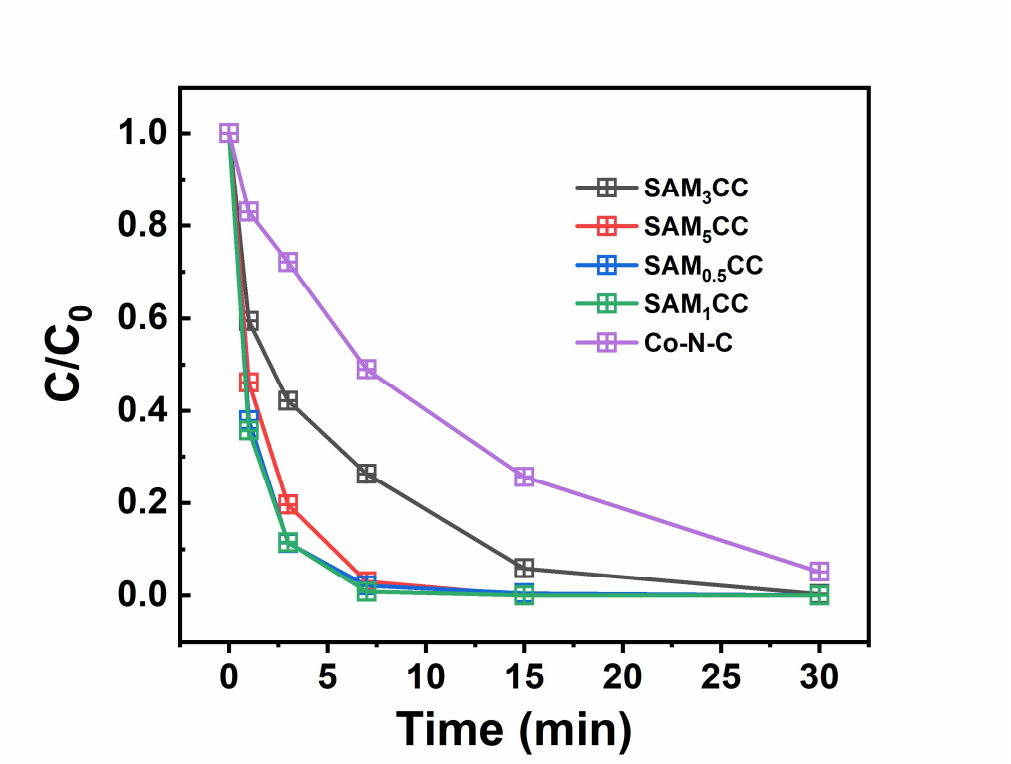

Fig. S2. Degradation activity of catalysts with different molar ratios of $(NH_4)_2MoO_4$ to $Co(Ac)_2$, and the dosage of o-phenanthroline was kept at three times of the total of $Co(CH_3COO)_2$ and $(NH_4)_2MoO_4$. Dosage: Catalyst :30 mg; PMS: 20 mg; C_{phenol}: 20 mg/L.

For the synthesis of SAM_xCC, the dosage of $Co(CH_3COO)_2$ was 62.5 mg. The dosage $(NH_4)_2MoO_4$ of was 0.0005x mol and the molar amount of 1,10-phenanthroline was 3 times of the total of $Co(CH_3COO)_2$ and $(NH_4)_2MoO_4$. From the data in the graph, it can be concluded that the best degradation activity of the catalyst was $SAM_{0.5}CC$. At this point, the amount of $(NH_4)_2MoO_4$ was 4.9 mg and the amount of o-phenanthroline was 148.5mg, which was consistent with the optimal dosage obtained in Fig. S1. Combining with the result in the Fig. S1, the catalyst synthesized by 62.5 mg $Co(CH_3COO)_2$, 4.9 mg $(NH_4)_2MoO_4$ and 148.5 mg o-phenanthroline was the most efficiently, and it was named as $SAMCC_{0.5}$ in the end. $SAMCC_{0.5}$ mentioned in the main text was this catalyst.

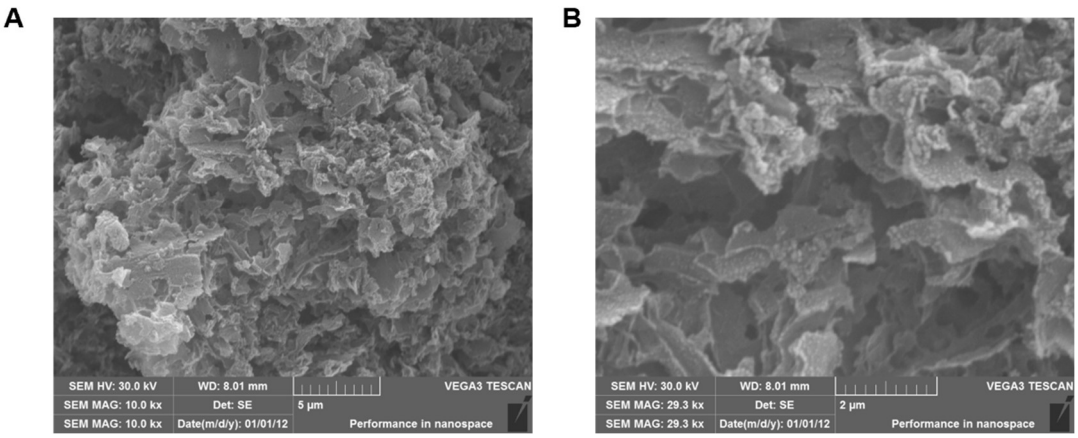

Fig. S3. SEM images of $SAMCC_{0.5}$. A and B, SEM images of $SAMCC_{0.5}$.

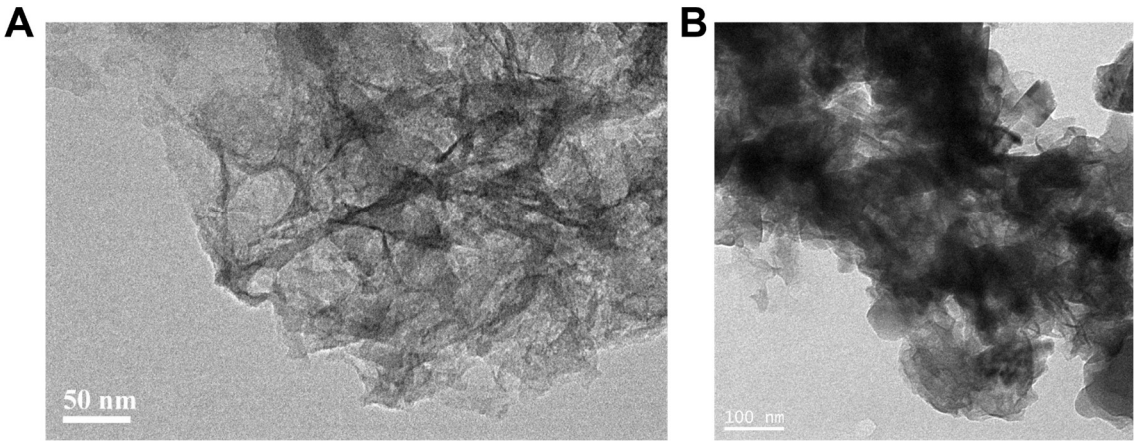

Fig. S4. *A* and *B,* HRTEM images of $SAMCC_{0.5}$.

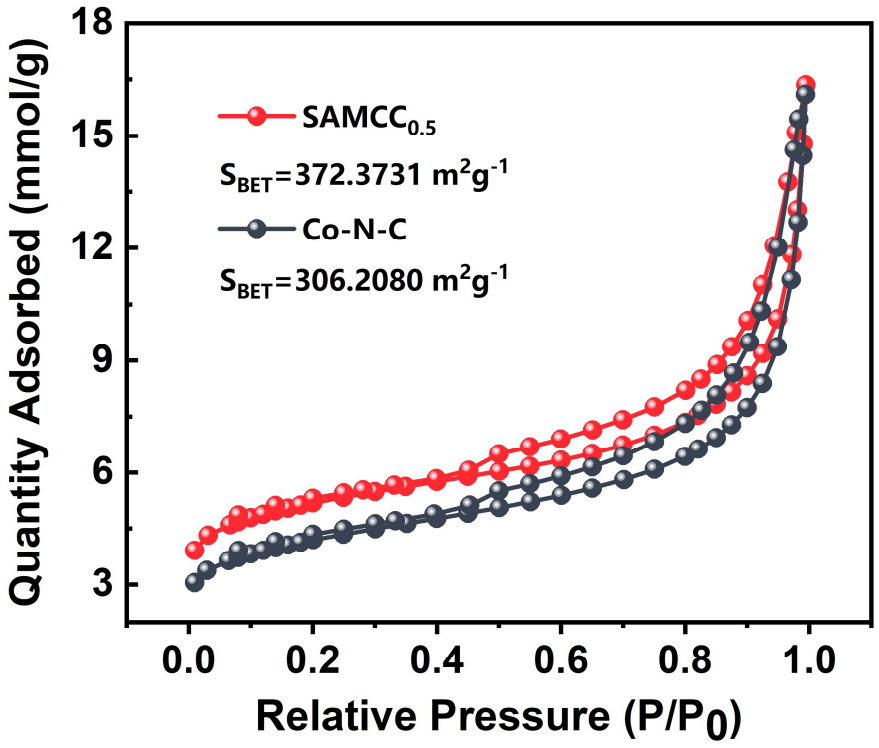

Fig. S5. Specific surface area of $SAMCC_{0.5}$. Nitrogen adsorption and desorption isotherms of $SAMCC_{0.5}$ and Co-N-C.

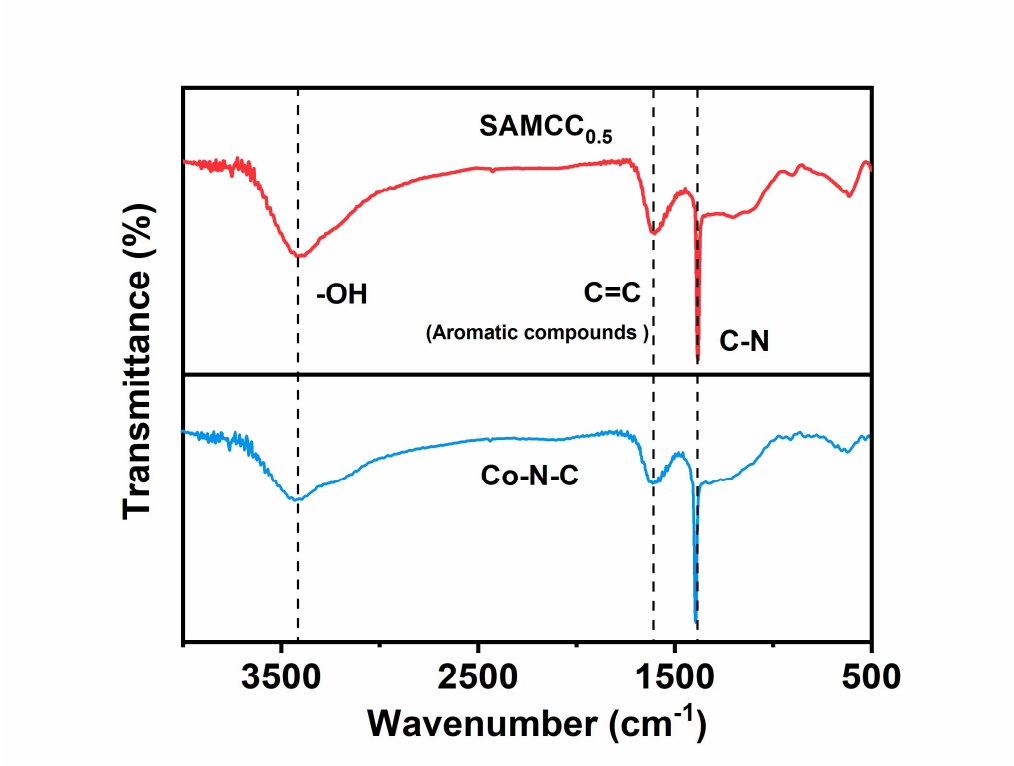

Fig. S6. Infrared spectroscopy of $SAMCC_{0.5}$ and Co-N-C.

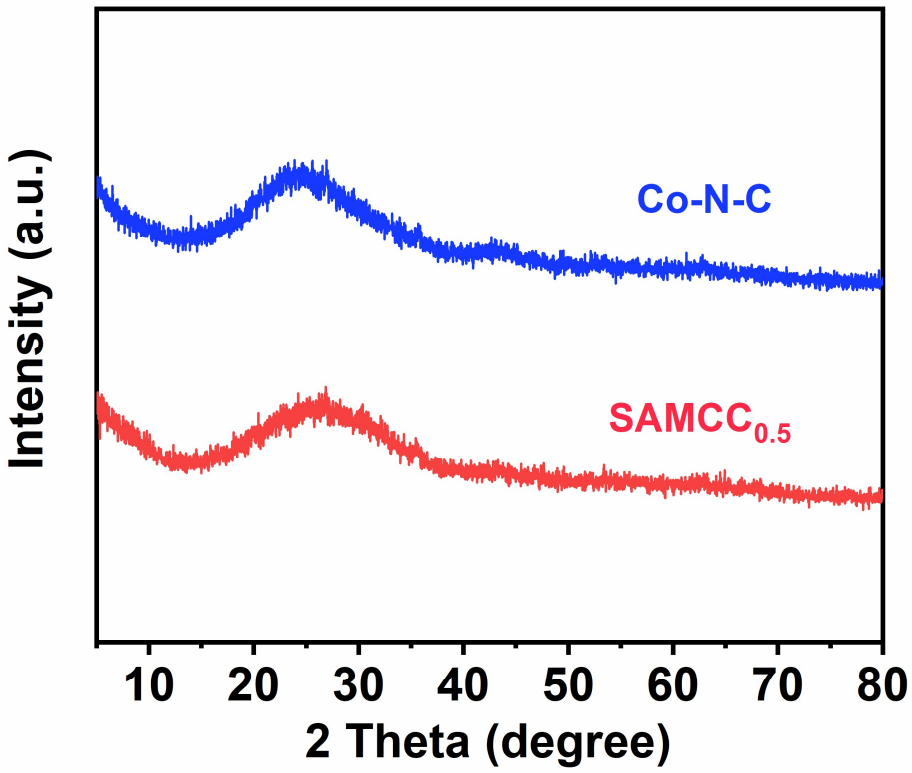

Fig. S7. XRD pattern of $SAMCC_{0.5}$ and Co-N-C.

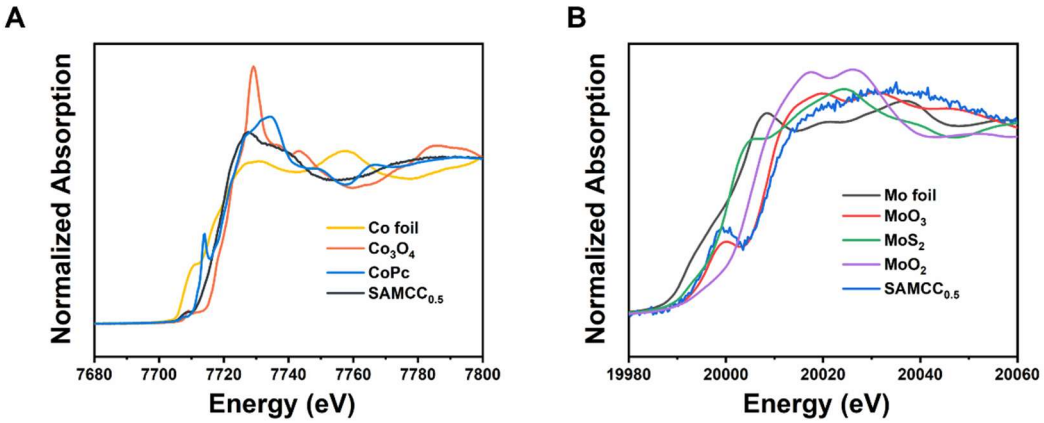

Fig. S8. XANES of $SAMCC_{0.5}$. *A*, XANES of Co element in $SAMCC_{0.5}$. *B*, XANES of Mo element in $SAMCC_{0.5}$.

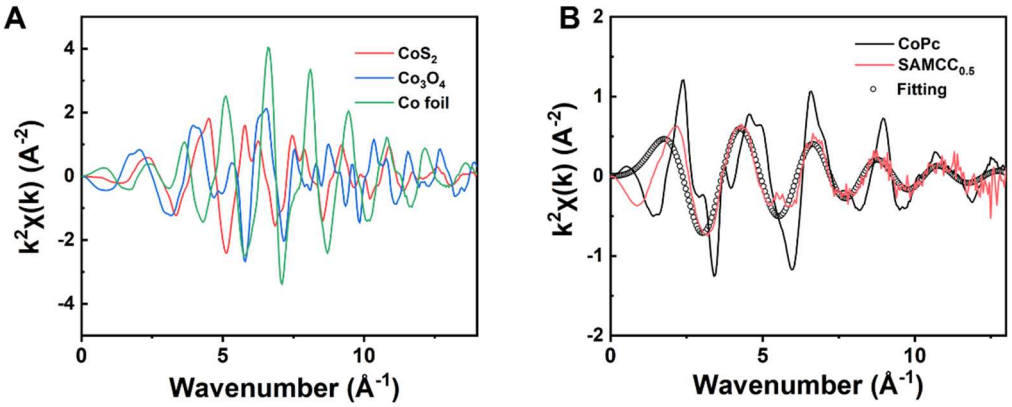

Fig. S9. EXAFS of Co element in k-space and corresponding fitting curves. *A*, EXAFS in k-space for CoS_2, Co_3O_4 and Co foil. *B*, EXAFS in k-space for CoPc, $SAMCC_{0.5}$ and Fitting curve.

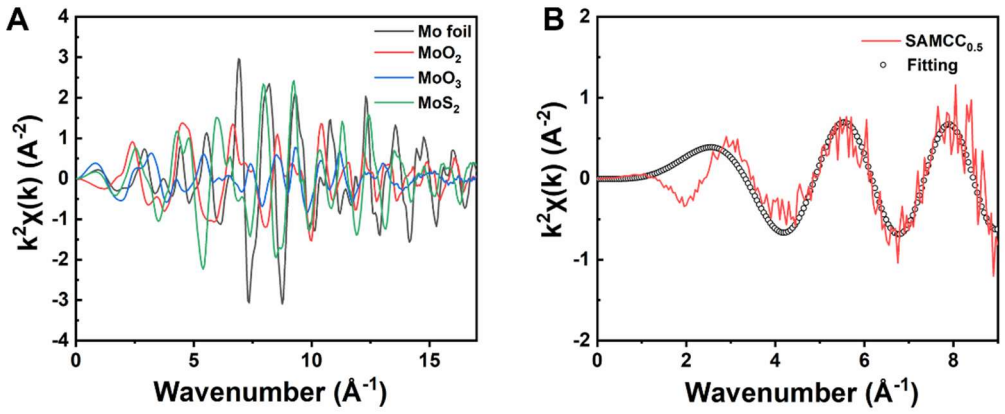

Fig. S10. EXAFS of Mo element in k-space and corresponding fitting curves. *A*, EXAFS in k-space for MoS_2, MoO_3, MoO_2 and Co foil. *B*, EXAFS in k-space for $SAMCC_{0.5}$ and Fitting curve.

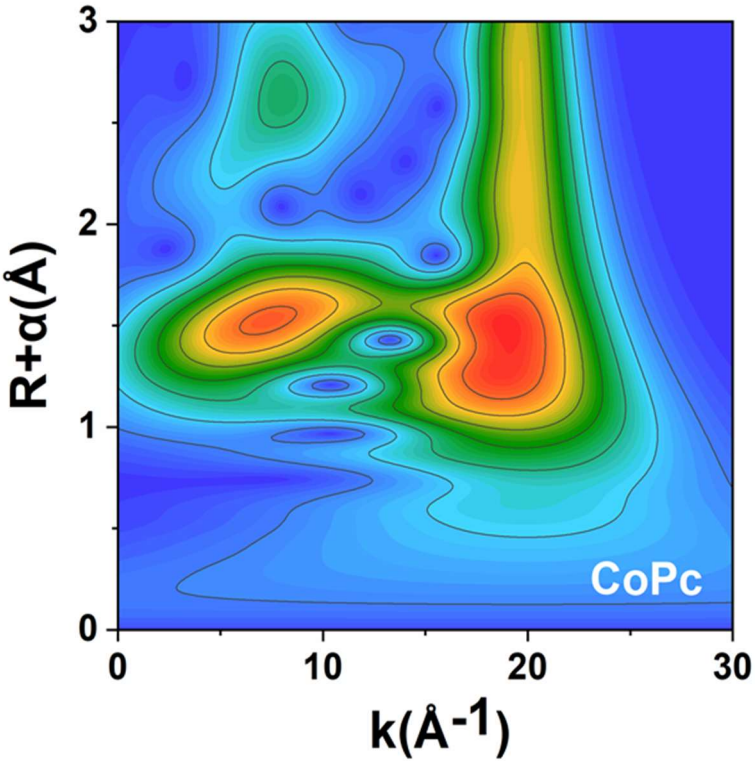

Fig. S11. EXAFS of CoPc in k-space after being k^3-weighted Fourier-transformed.

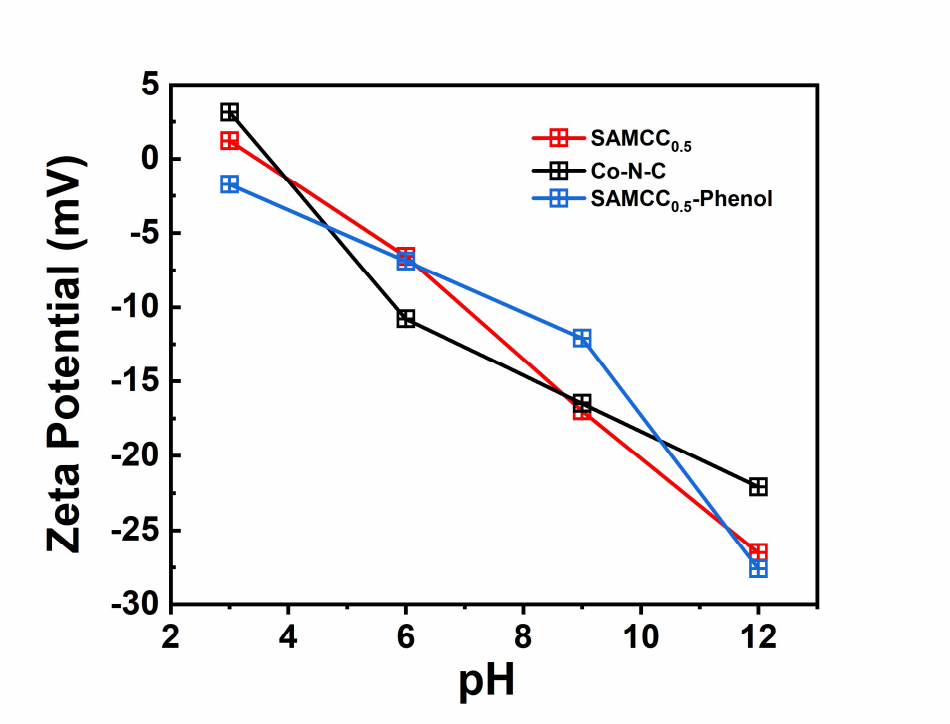

Fig. S12. EXAFS of CoPc in k-space after being k^3-weighted Fourier-transformed.

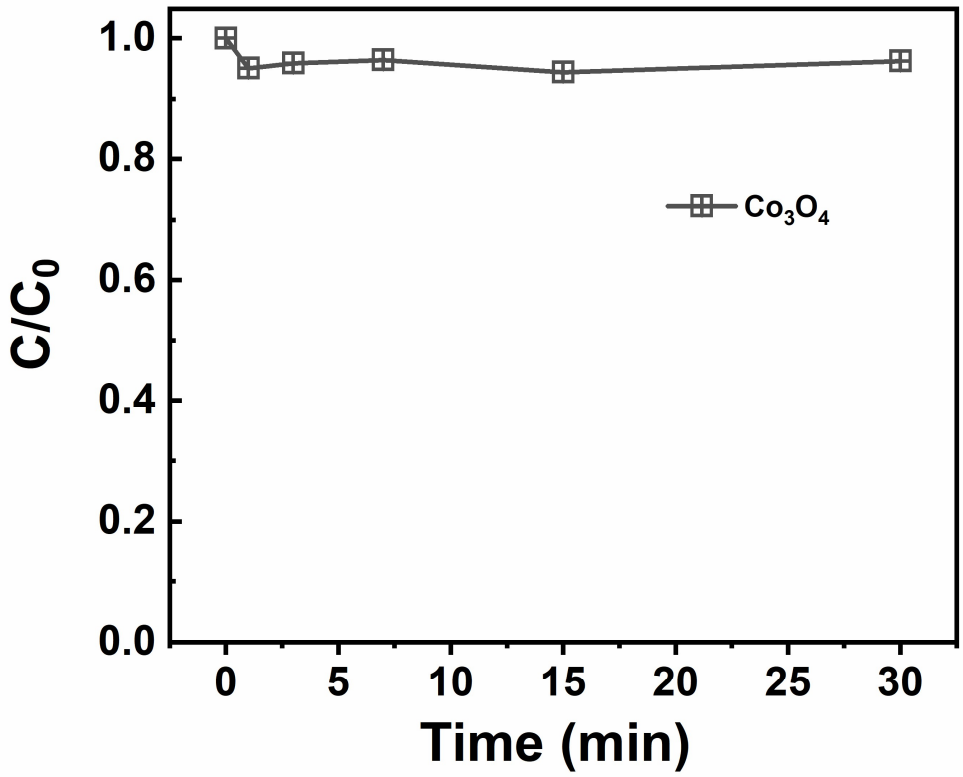

Fig. S13. Degradation rate of phenol with Co_3O_4 as catalyst. Dosage: Co_3O_4 :7 mg; PMS: 20 mg; C_{phenol}: 20 mg/L; reaction resolution: 100 mL deionized water.

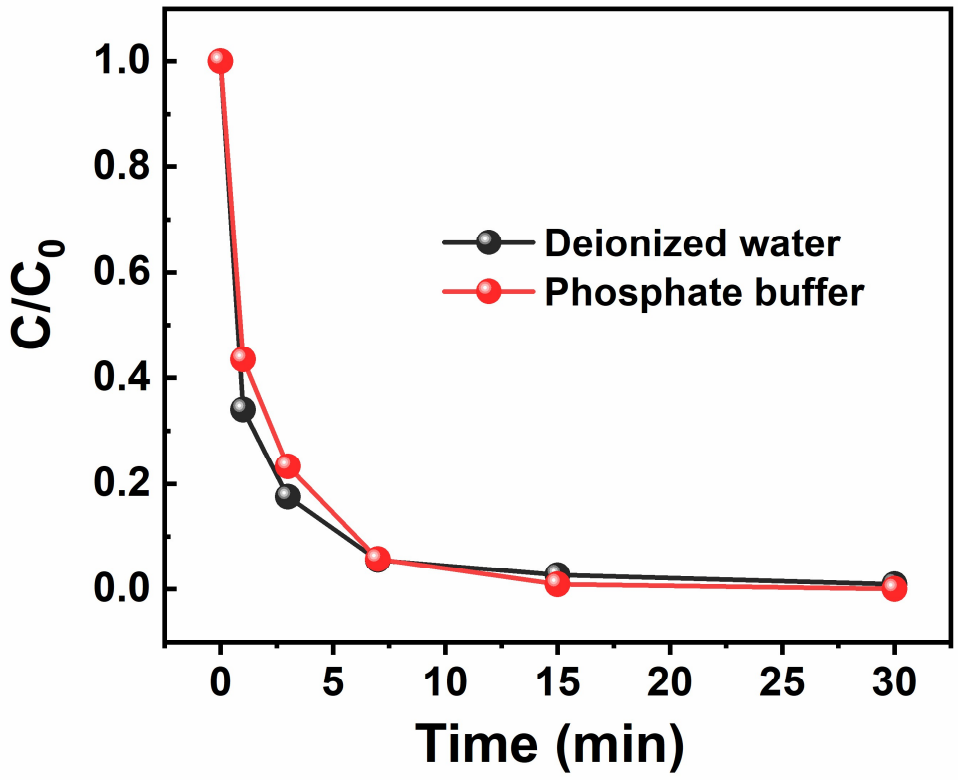

Fig. S14. Degradation rate of phenol in the phosphate buffer (pH=6.86) and deionized water with $SAMCC_{0.5}$ as catalyst. Dosage: $SAMCC_{0.5}$:30 mg; PMS: 20 mg; C_{phenol}: 20 mg/L; reaction resolution: 100 mL deionized water.

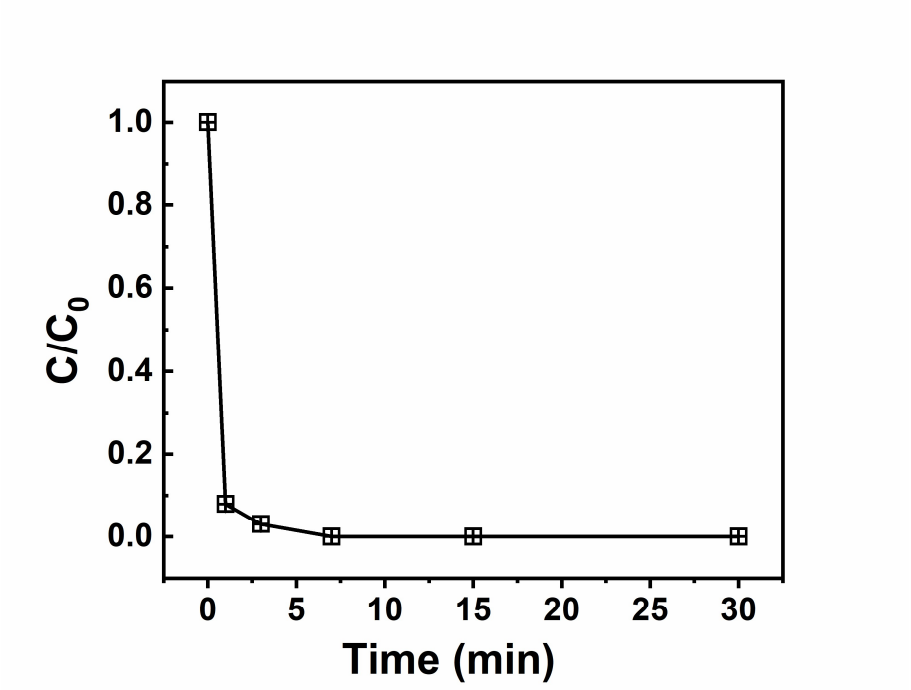

Fig. S15. Degradation rate of phenol with $SAMCC_{0.5}$ as catalyst when humic acid was present in the system. Dosage: $SAMCC_{0.5}$:30 mg; PMS: 20 mg; C_{phenol}: 20 mg/L.

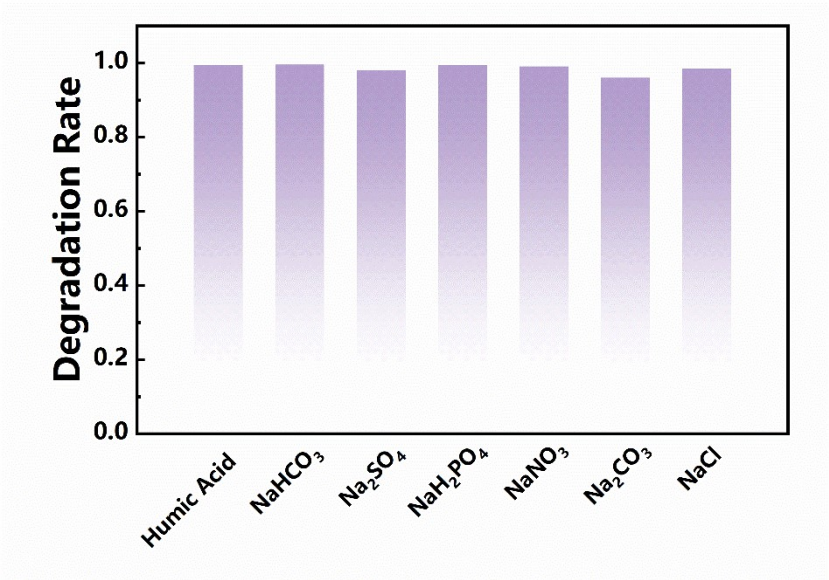

Fig. S16. Degradation rate of phenol in the phosphate buffer with different anions added. Dosage: $SAMCC_{0.5}$:30 mg; PMS: 20 mg; C_{phenol}: 20 mg/L.

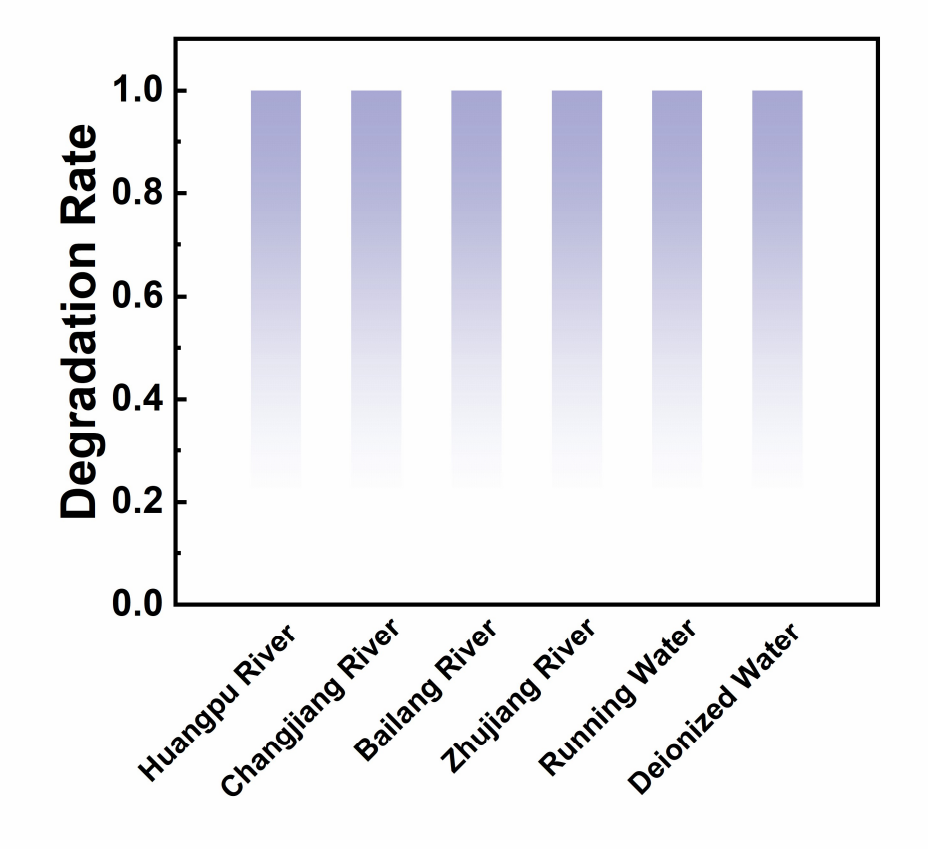

Fig. S17. Degradation rate of phenol with different solution from different river. Dosage: $SAMCC_{0.5}$:30 mg; PMS: 20 mg; C_{phenol}: 20 mg/L.

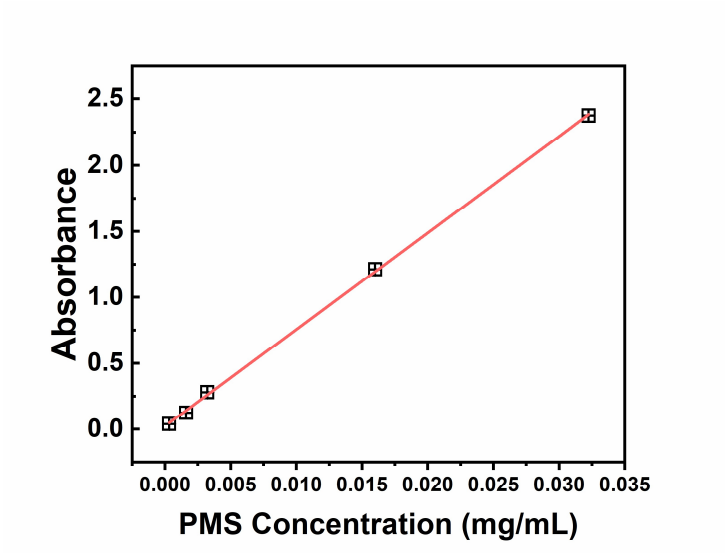

Fig. S18. Linear relationship between the concentration of PMS and the absorbance of solution in the detection process and the related fitting curve.

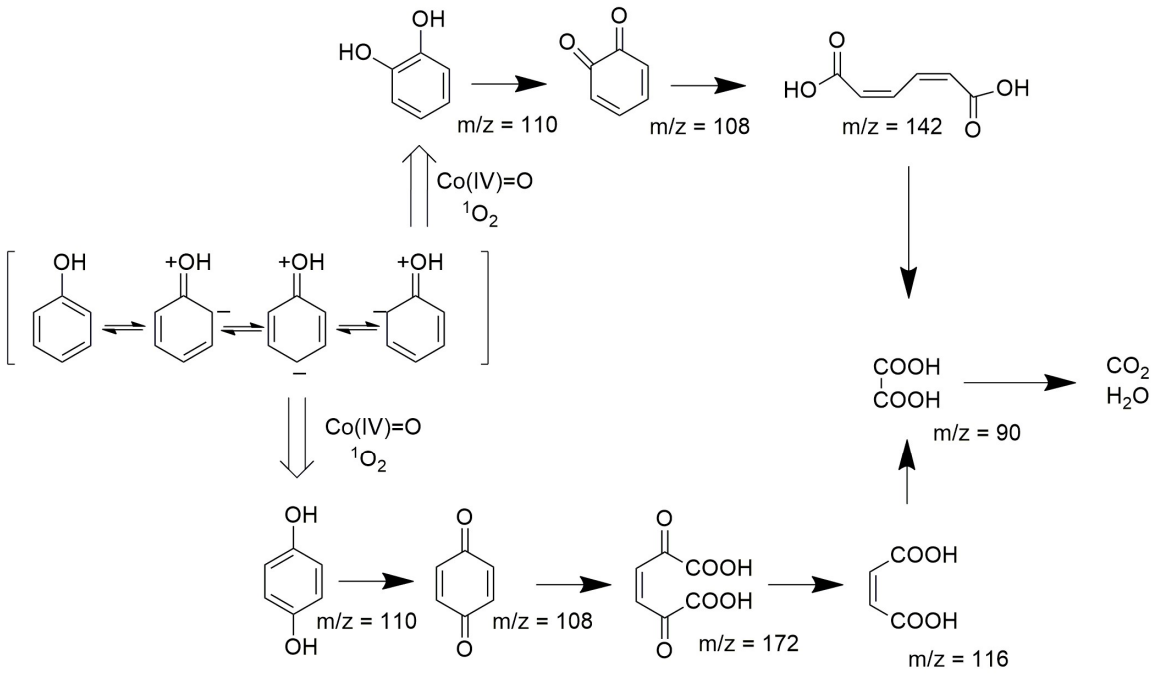

Fig. S19. Possible pathway for degradation of phenol by SAMCC$_{0.5}$-PMS system.

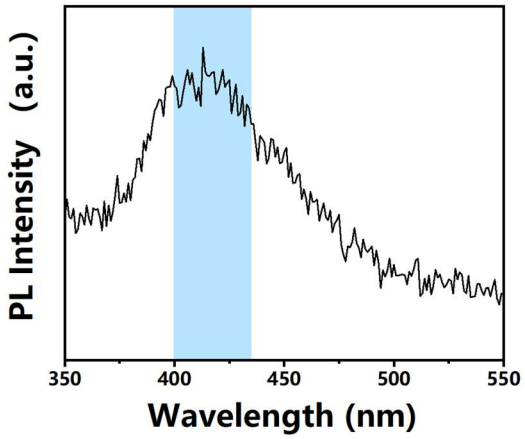

Fig. S20. Using benzoic acid as probe, hydroxyl radical was determined by fluorescence method. Dosage: $SAMCC_{0.5}$:30 mg; PMS: 20 mg; $C_{benzoic\ acid}$: 20 mg/L.

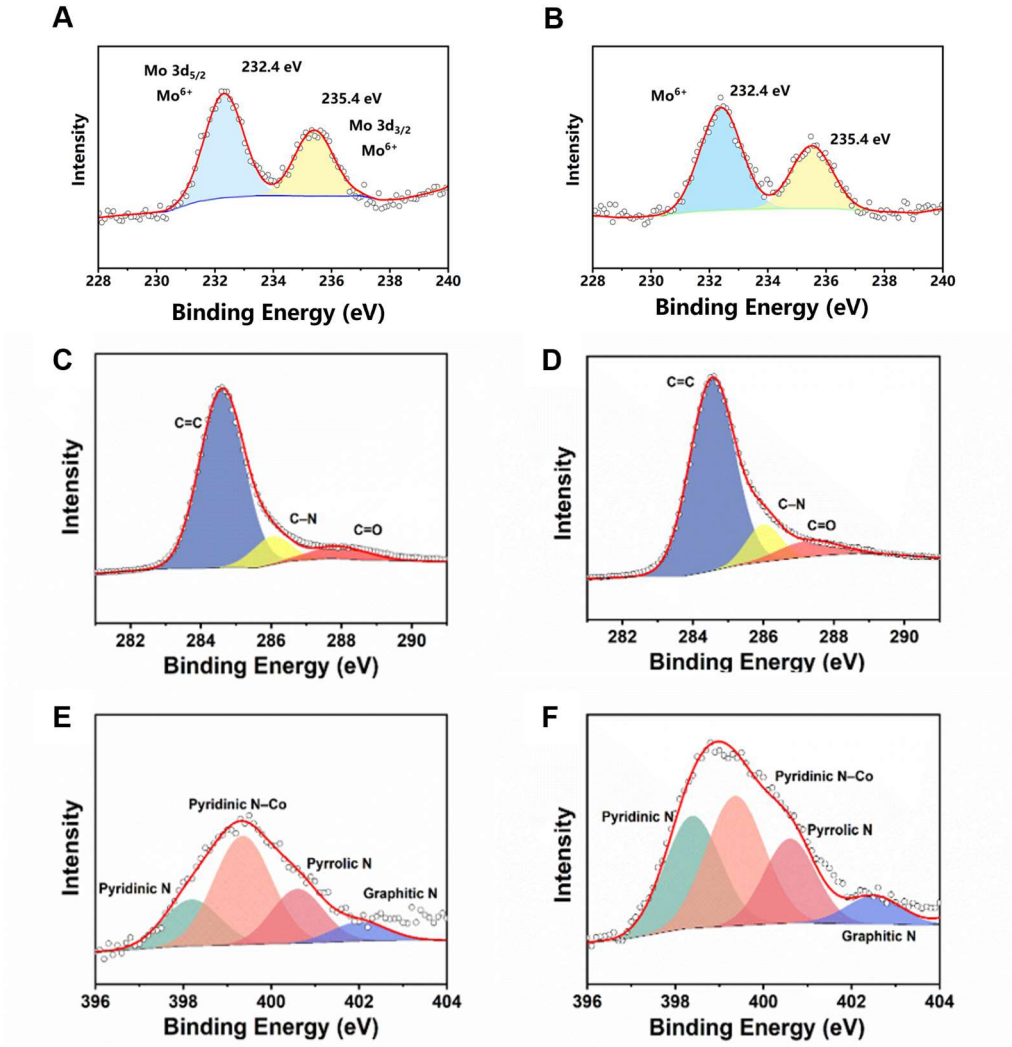

Fig. S21. XPS results of $SAMCC_{0.5}$ before and after reaction. *A,B* XPS results of Mo element of $SAMCC_{0.5}$ before and after reaction. *C,D* XPS results of C element of $SAMCC_{0.5}$ before and after reaction. *E,F* XPS results of N element of $SAMCC_{0.5}$ before and after reaction.

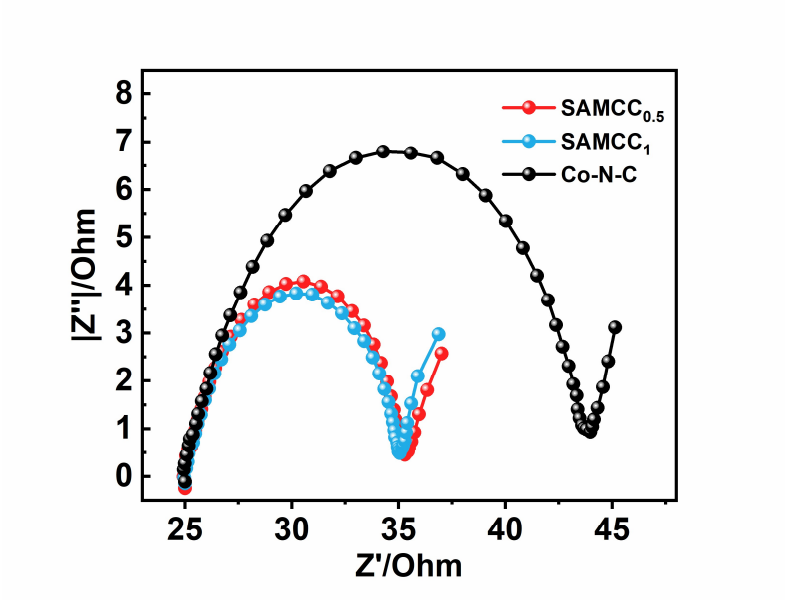

Fig. S22. Electrochemical impedance spectroscopy (EIS) of $SAMCC_1$, $SAMCC_{0.5}$ and Co-N-C.

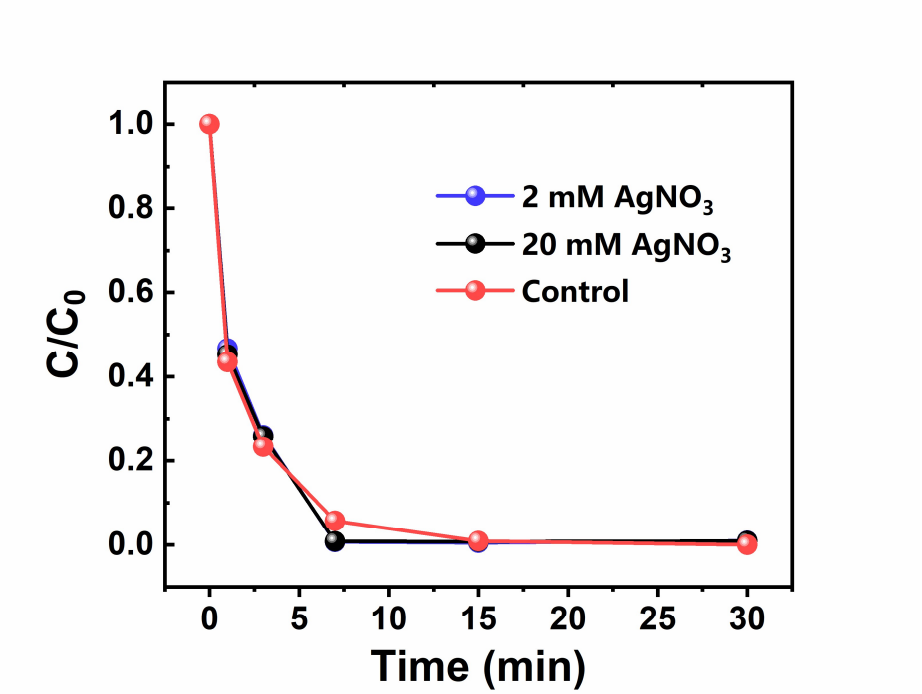

Fig. S23. $AgNO_3$ sacrificial agent experiments. Dosage: catalyst: 300 mgL^{-1} $SAMCC_{0.5}$, PMS: 200 mgL^{-1}, aqueous solution: 100 mL, reaction time: 30 min.

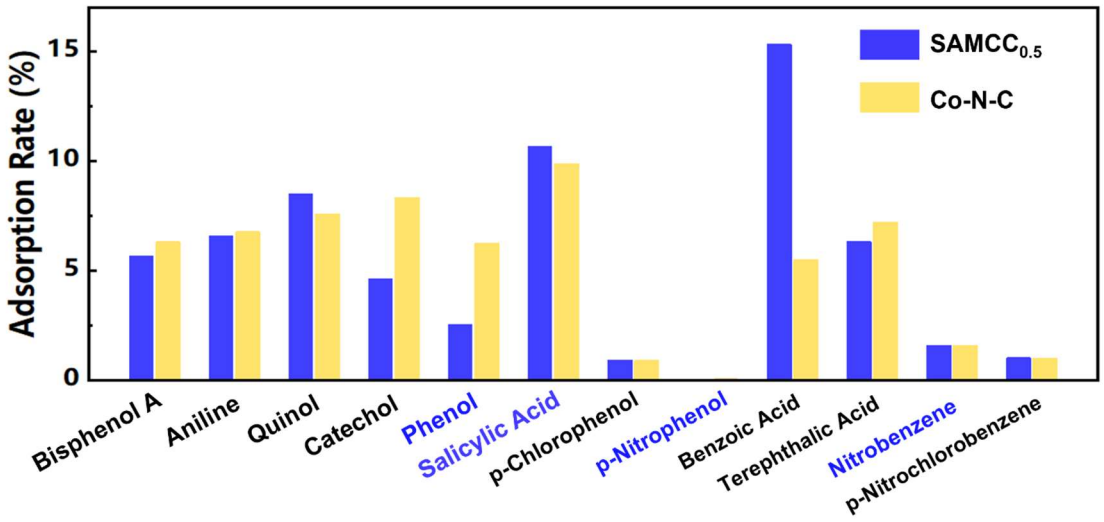

Fig. S24. Adsorption rate of different model pollutants in the comparison between $SAMCC_{0.5}$ and Co-N-C. Dosage: catalyst: 300 mgL^{-1}, aqueous solution: 100 mL, reaction time: 5 min.

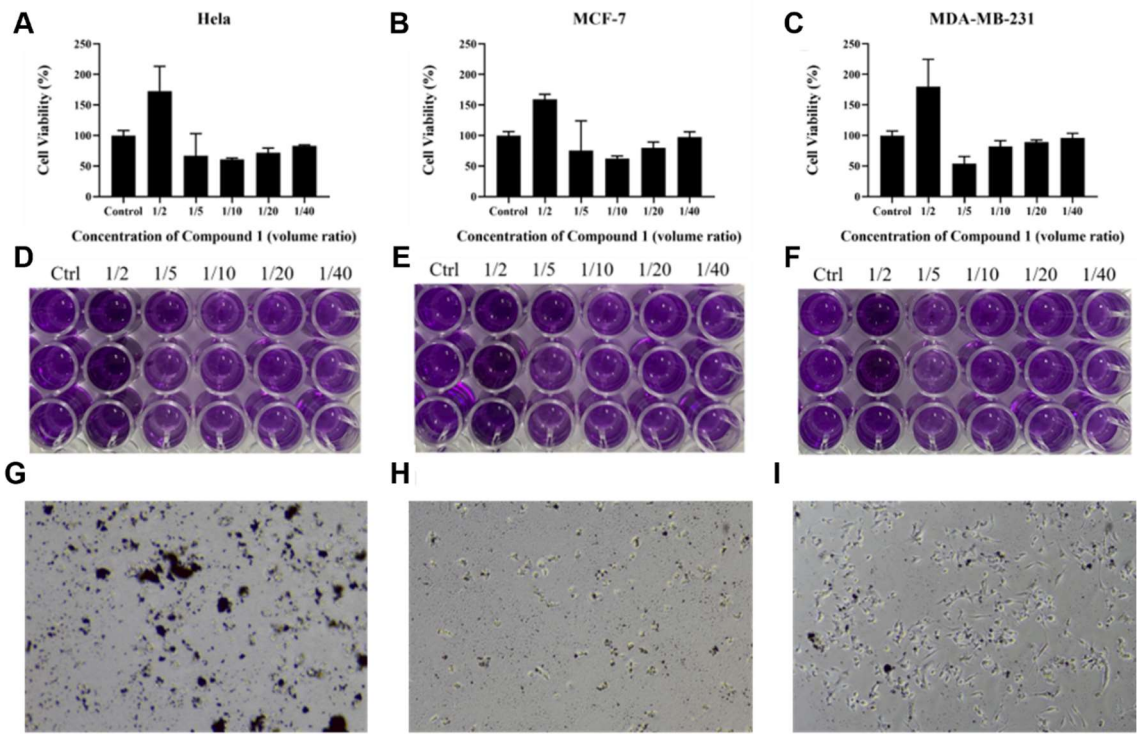

Fig. S25. Biotoxicity tests of $SAMCC_{0.5}$. *A,B,C,* Cell viability of Hela / MCF-7 / MDA-MB-231 cell lines at different $SAMCC_{0.5}$ concentrations. 1/2, 1/5, 1/10, 1/20 and 1/40 were respectively corresponding to 1500, 600, 300, 150 and 75 mg/L $SAMCC_{0.5}$. Cell culture time: 48 h. *D,E,F,* Concentration of viable cells with 0.5 mg/mL 3-(4,5-dimethylthiazol-2-yl)-2,5-diphenyltetrazolium bromide (MTT) as inspection agent. *G,H,J,* Cells in the culture medium were observed under a microscope (10×10 time).

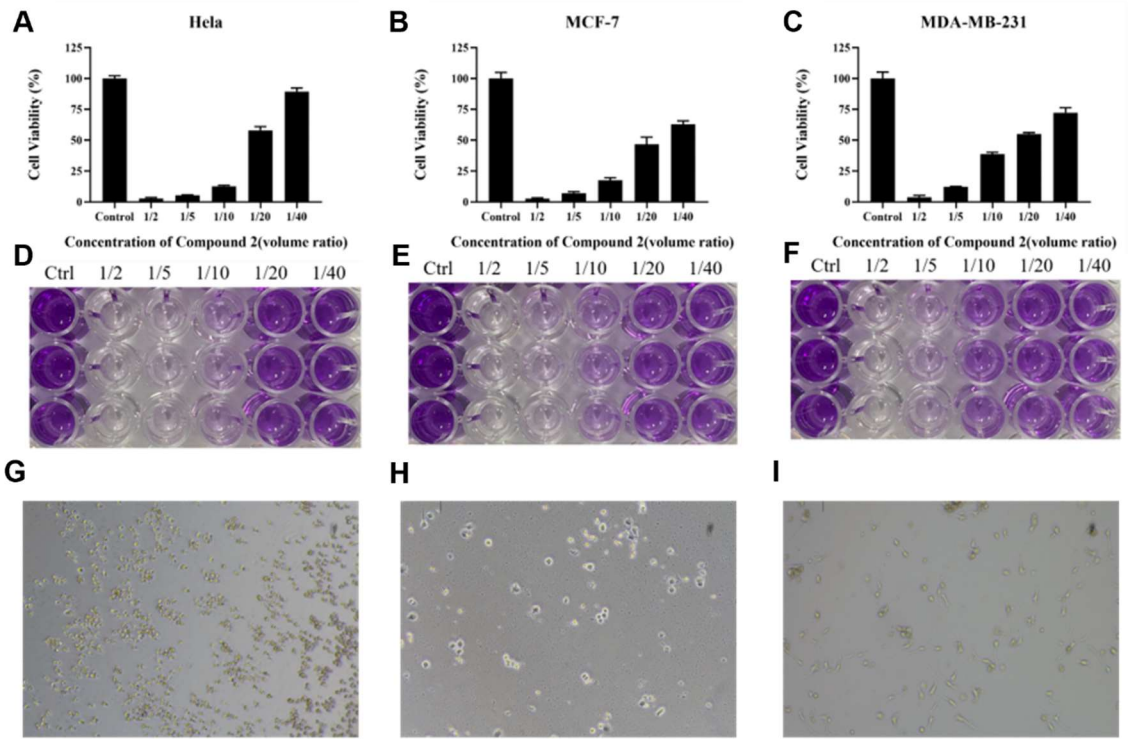

Fig. S26. Biotoxicity tests of $CoCl_2$. *A,B,C,* Cell viability of Hela / MCF-7 / MDA-MB-231 at different $CoCl_2$ concentrations. 1/2, 1/5, 1/10, 1/20 and 1/40 were respectively corresponding to 11.1, 4.44, 2.22, 1.11 and 0.555 mg/L $CoCl_2$. Cell culture time: 48 h. *D,E,F,* Concentration of viable cells with 0.5 mg/mL 3-(4,5-dimethylthiazol-2-yl)-2,5-diphenyltetrazolium bromide (MTT) as inspection agent. *G,H,J,* Cells in the culture medium were observed under a microscope (10×10 time). Compared with $SAMCC_{0.5}$, $CoCl_2$ showed stronger biotoxicity to Hela / MCF-7 / MDA-MB-231 cell lines.

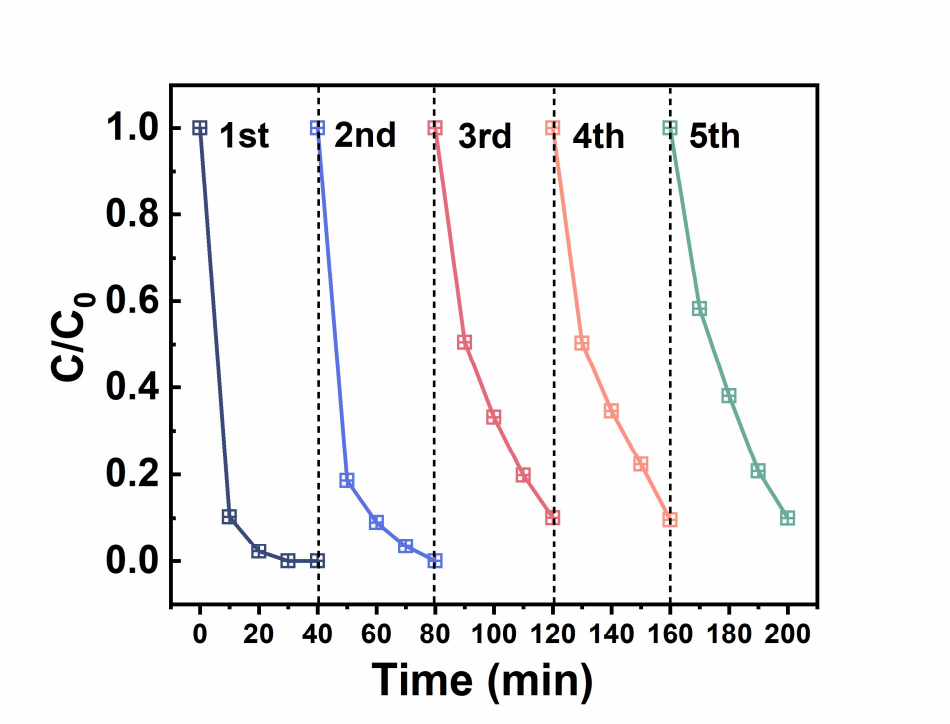

Fig. S27. 5 rounds cycle experiment for $SAMCC_{0.5}$.

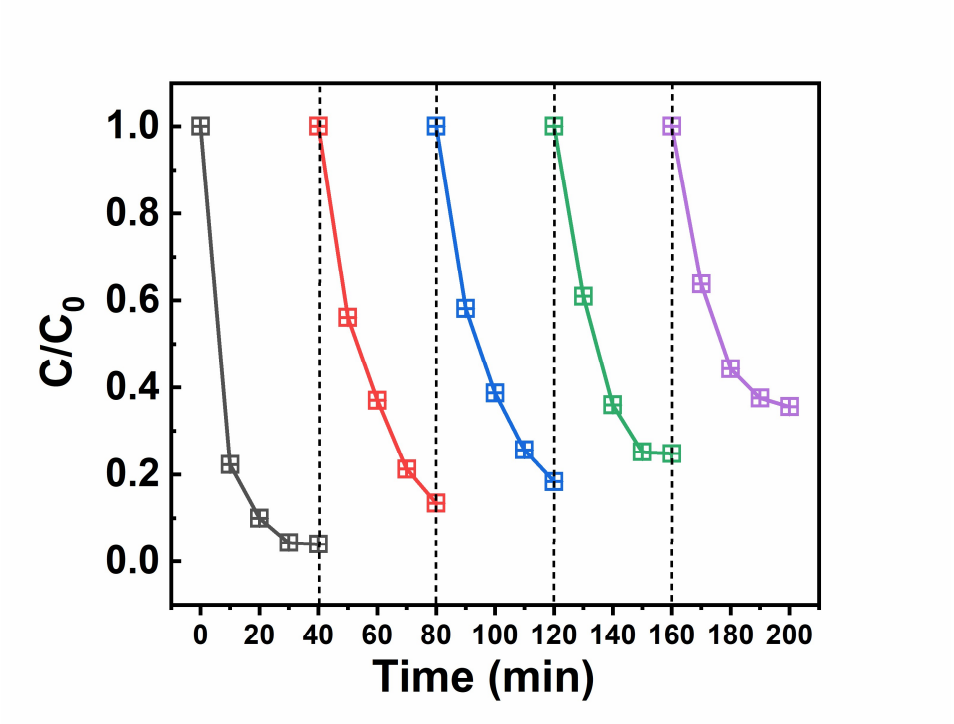

Fig. S28. 5 rounds cycle experiment for Co-N-C.

Table S1. Mass proportion of Co and Mo elements in catalyst obtained through inductively coupled plasma atomic emission spectrometry (ICP-AES).

Sample	Co%	Mo%
$SAMCC_{0.5}$	0.74	0.19
Co-N-C	1.00	/

Table S2. Conversion of (E)-1,2-Diphendiene and selectivity of 2, 3-Diphenyloxirane in $SAMCC_{0.5}$-PMS, Co-N-C-PMS, $CoCl_2$-PMS systems.

Sample	(E)-1,2-Diphendiene Conversion (%)	2, 3-Diphenyloxirane Selectivity (%)
$SAMCC_{0.5}$	23.6	18.2
Co-N-C	12.4	25.3
$CoCl_2$	100	1.31

Table S3. The concentration of cobalt ions and molybdenum in the solution of $SAMCC_{0.5}$-PMS system, $CoCl_2$-PMS system, Co-N-C-PMS system, Mo-N-C-PMS system. Dosage: PMS: 200 mgL^{-1}; Catalyst: 300 mgL^{-1} $SAMCC_{0.5}$, Co-N-C and Mo-N-C, 22.2 mgL^{-1} $CoCl_2$; Phenol: 20 mgL^{-1}; Reaction resolution: 100 mL.

Sample	Co (mg/L)	Mo (mg/L)
$SAMCC_{0.5}$	0.39	0.20
$CoCl_2$	20.10	/
Co-N-C	0.63	/
Mo-N-C	/	2.5

Table S4. $SAMCC_{0.5}$-PMS system for treating actual wastewater. Dosage: Catalyst: 300 mgL^{-1} $SAMCC_{0.5}$; Reaction resolution: 100 mL.

Sample	COD before treatment (mg/L)	COD after treatment (mg/L)	Degradation Rate(%)
Biochemical Wastewater	277	150	45.84
Wastewater From BCEG	170	75	55.88

References

1. Kresse G, Furthmüller J. Efficiency of ab-initio total energy calculations for metals and semiconductors using a plane-wave basis set. *Comput. Mater. Sci.* **6**, 15-50 (1996).

2. Kresse G, Furthmüller J. Efficient iterative schemes for ab initio total-energy calculations using a plane-wave basis set. *Phys. Rev. B.* **54**, 11169 (1996).

3. Perdew JP, Burke K, Ernzerhof M. Generalized gradient approximation made simple. *Phys. Rev. Lett.* **77**, 3865 (1996).

4. Kresse G, Joubert D. From ultrasoft pseudopotentials to the projector augmented-wave method. *Phys. Rev. B* **59**, 1758 (1999).

5. Blöchl PE. Projector augmented-wave method. *Phys. Rev. B.* **50**, 17953 (1994).

6. Grimme S, Antony J, Ehrlich S, Krieg H. A consistent and accurate ab initio parametrization of density functional dispersion correction (DFT-D) for the 94 elements H-Pu. *J. Chem. Phys.* **132**, 154104 (2010).

7. Grimme S, Ehrlich S, Goerigk L. Effect of the damping function in dispersion corrected density functional theory. *J. Comput. Chem.* **32**, 1456-1465 (2011).